Ondrej Zitka[1,2]
Sona Krizkova[1,3]
Ludmila Krejcova[1,3]
David Hynek[1,3]
Jaromir Gumulec[1,4]
Michal Masarik[1,3,4]
Jiri Sochor[1,3]
Vojtech Adam[1,3]
Jaromir Hubalek[1,2,3]
Libuse Trnkova[1,3,5]
Rene Kizek[1,3,5]

[1]Department of Chemistry and Biochemistry, Faculty of Agronomy, Mendel University in Brno, Brno, Czech Republic
[2]Department of Microelectronics, Faculty of Electrical Engineering and Communication, Brno University of Technology, Brno, Czech Republic
[3]Central European Institute of Technology, Brno University of Technology, Brno, Czech Republic
[4]Department of Pathological Physiology, Faculty of Medicine, Masaryk University, Brno, Czech Republic
[5]Department of Chemistry, Faculty of Science, Masaryk University, Brno, Czech Republic

Received August 3, 2011
Revised August 15, 2011
Accepted August 15, 2011

Research Article

Microfluidic tool based on the antibody-modified paramagnetic particles for detection of 8-hydroxy-2′-deoxyguanosine in urine of prostate cancer patients

Guanosine derivatives are important for diagnosis of oxidative DNA damage including 8-hydroxy-2′-deoxyguanosine (8-OHdG) as one of the most abundant products of DNA oxidation. This compound is commonly determined in urine, which makes 8-OHdG a good non-invasive marker of oxidation stress. In this study, we optimized and tested the isolation of 8-OHdG from biological matrix by using paramagnetic particles with an antibody-modified surface. 8-OHdG was determined using 1-naphthol generated by alkaline phosphatase conjugated with the secondary antibody. 1-Naphthol was determined by stopped flow injection analysis (SFIA) with electrochemical detector using a glassy carbon working electrode and by stationary electrochemical detection using linear sweep voltammetry. A special modular electrochemical SFIA system which needs only 10 μL of sample including working buffer for one analysis was completely designed and successfully verified. The recoveries in different matrices and analyte concentration were estimated. Detection limit (3 S/N) was estimated as 5 pg/mL of 8-OHdG. This method promises to be very easily modified to microfluidic systems as ''lab on valve''. The optimized method had sufficient selectivity and thus could be used for determination of 8-OHDG in human urine and therefore for estimation of oxidative DNA damage as a result of oxidation stress in prostate cancer patients.

Keywords:
Electrochemistry / ELISA / Magnetic particles / Nanoseparation
DOI 10.1002/elps.201100430

1 Introduction

Studies over the last decade have demonstrated that reactive oxygen species (ROS) and reactive nitrogen species (RNS) actively participate in a diverse array of pathological and physiological processes, including normal cell growth, induction and maintenance of the transformed state, programmed cell death and cellular senescence on the one side, and damaging of cell membranes, cell compartments, peptides, proteins and nucleic acids on the other side [1, 2]. One may suggest that oxidative stress represents an imbalance between the production ROS and a biological system's ability to readily detoxify the reactive intermediates, to repair the resulting damage or to utilize them in physiological processes. From above-mentioned negative events, oxidative DNA damage and consequent DNA mutation represented by elevated levels of 8-hydroxy-2′-deoxyguanosine (8-OHdG) belong to the most critical.

It is not surprising that 8-OHdG (Fig. 1) is considered as a biomarker of oxidative stress caused by various exogenous and endogenous events [3–7]. 8-OHdG can be determined in easily obtainable body fluids as saliva (oral cancer [8], periodontitis [9] and systemic sclerosis [10]), semen (indicator of sperm quality [11] and reduced fertility [12, 13]) and urine (various types of cancers [14–16], atherosclerosis [17], diabetes [18], Parkinson's [19], diabetes and Alzheimer's diseases [20]). In addition, there is also association between heavy metals action (e.g. arsenic, cadmium) to form ROS and/or RNS producing DNA lesions inclosing 8-OHdG occurrence, which leads to development of cancer

Correspondence: Dr. Rene Kizek, Department of Chemistry and Biochemistry, Mendel University in Brno, Zemedelska 1, CZ-613 00 Brno, Czech Republic
E-mail: kizek@sci.muni.cz
Fax: +420-5-4521-2044

Abbreviations: 8-OHdG, 8-hydroxy-20-deoxyguanosine**; FIA-ED,** flow injection analysis with amperometric detection**; ED,** electrochemical detector**; GCE,** glassy carbon electrode**; LSV,** linear sweep voltammetry**; MPs,** paramagnetic or superparamagnetic particles/beads**; RAM-AP,** rabbit anti-mouse immunoglobulin modified by alkaline phosphatase**; RNS,** reactive nitrogen species**; ROS,** reactive oxygen species**; RSD,** relative standard deviation**; SFIA,** stopped flow injection analysis**; SFIA-ED,** stopped flow injection analysis with electrochemical detection

Colour Online: See the article online to view Figs. 1–8 in colour.

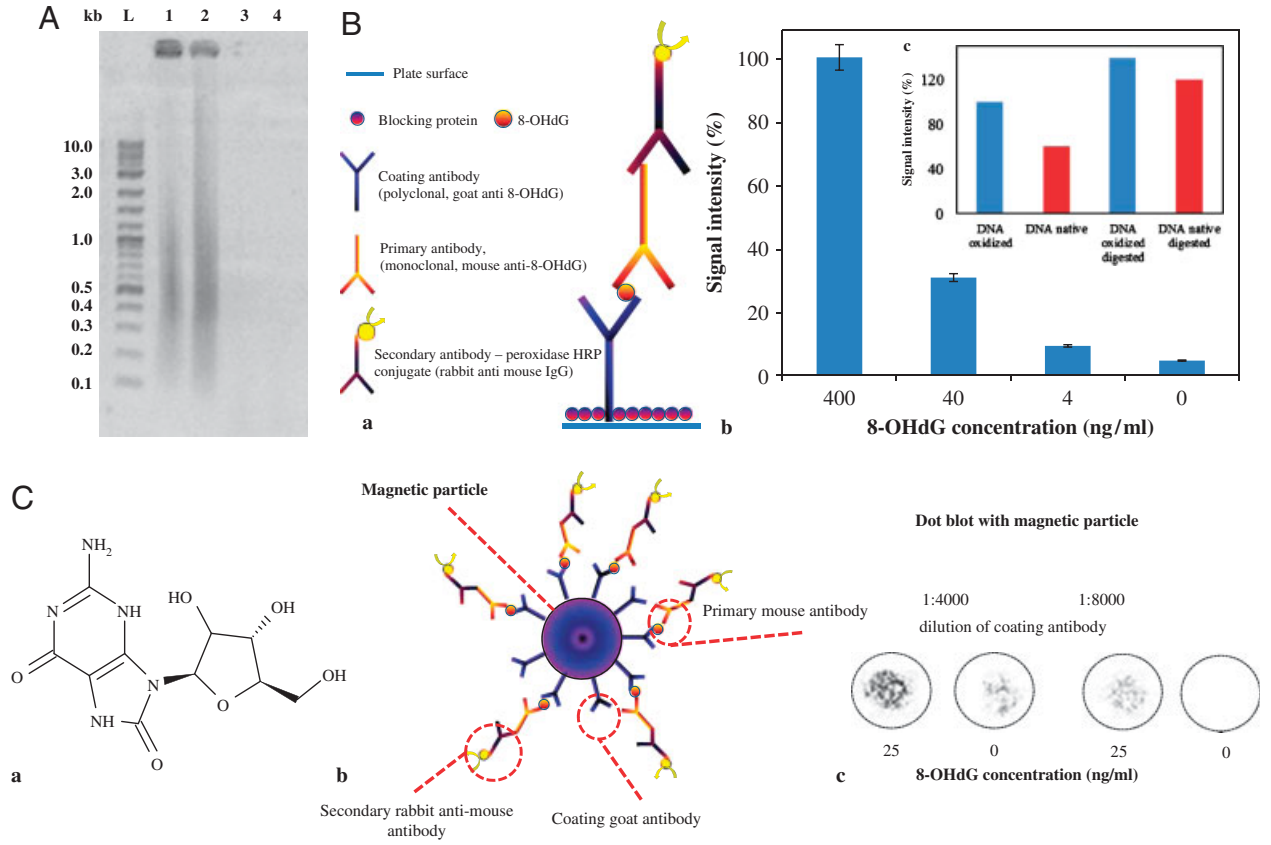

Figure 1. DNA samples were analyzed on a 1% agarose gel. L–2-log DNA ladder (New England Biolabs, USA), 1–1.7 μg of DNA oxidized with UV irradiation and H_2O_2; 2–1.7 μg of control DNA; 3–1.7 μg of oxidized DNA digested with nuclease from. *S. aureus*; 4–1.7 μg of oxidized DNA digested with nuclease from. *S. aureus*; digestion: DNAse from *S. aureus*, 0.02 U per mg of DNA (A). Simplified scheme of ELISA detection of 8-OHdG (Ba). Comparison of ELISA signal intensity of 400, 40, 4 and 0 ng/mL 8-OHdG in presence of 1.41 μM concentration of adenine, thymine, cytosine and guanine (Bb). Comparison of ELISA signal intensity for native/oxidized and digested native/oxidized DNA, DNA 1 mg/mL, UV irradiation 3 h (Bc). Chemical structure of 8-OHdG (Ca). Simplified scheme of magnetic beads ELISA detection of 8-OHdG (Cb). Dot blot with magnetic beads in presence 1:4000 and 1:8000 polyclonal goat antibody and 0 and/or 25 ng/mL 8-OHdG. Magnetic beads were pipetted on a PVDF membrane. Chromogenic substrates for horseradish peroxidase was used (TMB – tetramethylbenzidine) in 0.5 M acetate buffer with 0.1% H_2O_2, pH 5.5), after the sufficient colouring the reaction was stopped by rinsing with water (Cc).

[21–28]. In 2008, the paper showing association of urinary level of nickel and acute leukaemia in Chinese children with significantly higher concentration of urinary 8-OHdG [29] was published. However, there is lack information about relationships between heavy metals, oxidative stress and molecules scavenging reactive radicals as reduced glutathione and/or metallothionein [30].

Due to clinical importance of 8-OHdG, this molecule is target for many bioanalytical, biochemical and biological tools and approaches. Chromatographic ones consisting of HPLC and MS belong to the most accurate analytical methods [31], however, these methods are laborious and time-consuming due to demands on pre-treatment of a sample [32]. On the other hand, coupling of HPLC with electrochemical detector (ED) seems to be very convenient for determination of 8-OHdG because of versatility of ED detector, which is ultrasensitive to this molecule and less sensitive to common impurities [33–36]. This fact can be well documented by numerous papers testing various working electrodes for this purpose. 8-OHdG was determined on glassy carbon electrode (GCE) with detection limit of 8×10^{-7} M [37]. The modification of GCE surface with multiwall carbon nanotubes decreased LOD down to 9×10^{-9} M [38]. This approach seems to have a great possibilities as shown GCE-modified carbon nanotubes dispersed in polyethylenimine with LOD of 1×10^{-7} M in the presence of its major interferences such as ascorbic and uric acid [39]. Except GCE, platinum, gold and SnO_2 electrodes were also tested for determination of 8-OHdG [40]. Due to trends to miniaturize analytical devices, activated carbon fibre microelectrodes were used as the sensing platform for measuring 8-OHdG in real time at the surface of a single lung epithelial cell under the influence of nicotine [41]. Such electrodes can be implemented in microfluidic systems fabricated by microelectromechanical systems (MEMS) technology, referred as ''lab-on-a-chip (LOC)'' or ''biochips'', carrying out entire protocols traditionally performed in a laboratory. Microfluidic immunoassays offer a promising combination

of simplicity, sensitivity and specificity of immunoassays and potential of miniaturization, automation and integration of microfluidic technologies [42].

There is a great research in coupling of miniaturized detectors with some separation techniques [43]. Paramagnetic or superparamagnetic particles/beads (MPs) represents promising tool in this field [44–46]. MPs, whose size is ranging from nm to mm, respond to external magnetic field and facilitate bioactive molecules binding because of their affinity for the MPs modified surface made of biologically components [47–50]. The paramagnetic properties of the particles enable us to use magnetic force for transferring of the beads or for rinsing of nonbinding, otherwise commonly interfering substances. Among other advantages of MPs belong easy-to-use, non-laborious relatively rapid sample preparation without centrifugation and dialysis compared to conventional purification techniques. The time needed to get target biomolecule is also reduced due to of the fact that binding of the biomolecule by MPs can protect it against physical and biological damage, e.g. denaturation [51]. The mostly used MPs in biosensors applications are superparamagnetic nanoparticles composed of ferrous oxide or ferric oxide [52]. Nanoparticles have a lot of physico-chemical advantages [53, 54]. Their size can be adapted to the extension and kind of a biological sample which is a source of target biomolecules (e.g. proteins 5–50 nm, viruses 20–450 nm, cells 10–100 μm) [55–59] and their surface can be modified by numerous substances including antibodies. Variety of polyclonal [60] and monoclonal [61, 62] antibodies against 8-OHdG have been prepared but they have not been used for modification of MPs to isolate 8-OHdG. In spite of this fact Enzyme-Linked ImmunoSorbent Assay (ELISA) is extensively used for determination of the target molecule [25, 33, 63, 64] and there are also available commercial kits [14, 62, 65–68]. However, there were observed some significant differences in the determined concentrations of 8-OHdG depending on a type of a sample type and used antibody [69]. Immunohistochemistry using antibodies to localize the antigen of interest in a tissue has been successfully utilized also for 8-OHdG determination in numerous types of tissues as gallbladder [70], liver [71], renal [61], hippocampus [72], breast [73], ovarian [74] and/or melanoma tissues [75]. In addition, immunoaffinity chromatography has been also tested for isolation of 8-OHdG with various types of subsequent detection [62, 76]. The main aim of this study was to design a microfluidic device for determination of 8-OHdG using sandwich immunoassay on the magnetic beads and electrochemical detection of the product of immunoassay as 1-naphthol.

2 Materials and methods

2.1 Chemicals and pH measurement

1-Naphthol, 1-naphthylphosphate and *p*-nitrophenyl phosphate, Na_2CO_3, $NaHCO_3$, BSA, human IgG, NaCl, Na_2PO_4 and $NaHPO_4$ were purchased from Sigma-Aldrich (USA). HPLC-grade methanol (>99.9%; v/v) was from Merck (Dortmund, Germany). Other chemicals were purchased from Sigma-Aldrich in ACS purity unless noted otherwise. Lyophilized highly polymerized DNA (Reanal, Hungary) was isolated from chicken erythrocytes (M_w = 400 000 g/mol). Stock standard solutions of 8-OHdG (1 mg/mL) were prepared with ACS water (Sigma-Aldrich) and stored in dark at −20°C. Working standard solutions were prepared daily by dilution of the stock solutions. The pH value was measured using WTW inoLab Level 3 with terminal Level 3 (Weilheim, Germany), controlled by the software MultiLab Pilot (Weilheim). The pH-electrode (SenTix H, pH 0–14/0–100°C/3 mol/L KCl) was regularly calibrated by set of WTW buffers (Weilheim). Polyclonal goat anti-8-OHdG and primary monoclonal mouse anti-8-OHdG antibodies were purchased from SantaCruz Biotechnology (USA). Polyclonal rabbit anti-mouse conjugate with alkaline phosphatase (AP-conjugated rabbit anti-mouse IgG) were purchased from Dako (Denmark). Magnetic microparticles Dynabeads Protein G were from Invitrogen (Norway). Nuclease from *Staphylococcus aureus* was purchased from Sigma-Aldrich. Plastic (tips, DWP plates) used was low retention and low protein binding and was purchased from Eppendorf (Germany).

2.2 ELISA

Coating polyclonal goat anti-8-OHdG antibodies diluted 1:10 000 in 0.05 M carbonate buffer (0.032 M Na_2CO_3 and 0.068 M $NaHCO_3$, pH 9.6) in volume of 100 μL per well were adsorbed on polystyrene 96-well microplate (Thermo Scientific, Nunc, Langenselbold, Germany) overnight at 4°C. The free surface of the wells was blocked with 1% m/v BSA in PBS (137 mM NaCl, 2.7 mM KCl, 1.4 mM NaH_2PO_4 and 4.3 mM Na_2HPO_4, pH 7.4) for 1 h at 37°C. Then, the wells were five times washed with PBS buffer containing 0.05% v/v Tween-20 (PBS-T). Further, 100 μL of 8-OHdG standard or sample per well was applied and the plate was incubated for 1 h at 37°C. After the five times washing of the wells with PBS-T, which was repeated after each step of the procedure, the plate was incubated with 100 μL of the mouse anti-8-OHdG primary antibody (1:1000 diluted) in 0.1% BSA-PBS for 1 h at 37°C. Then, the plate was incubated with 100 μL of rabbit anti-mouse secondary antibody labelled with horseradish peroxidase in dilution of 1:5000 in 1% BSA-PBS for 1 h at 37°C to visualize the interaction of 8-OHdG with the primary antibody. Dilutions of antibodies and incubation times were optimized (not shown). Prior to application of the chromogenic substrate the plate was incubated for 15 min with PBS. The mixture (100 μL) from the following substances (0.001% w/v of 3,3′,5,5′-tetramethylbenzidine (TMB) as substrate for horseradish peroxidase, 10 μL of hydrogen peroxide (30%, v/v), 0.5 mL of 2 M sodium acetate adjusted to pH 5.8 with 1 M citric acid and 10 mL of Milli-Q water) was applied to single well on the microplate. After the sufficient colouring (30 min

at 37°C) the reaction was stopped with 50 μL of 0.5 M H_2SO_4. The absorbance of the yellow product was measured at 450 nm using Multiscan EX microplate reader (Thermo Scientific). Measurements of the samples and standards were carried out in triplicates, in each plate the calibration curve and blind wells (with PBS instead sample) was included.

2.3 Dot-immunobinding assay

About 1 μL of the sample was pipetted on a PVDF membrane (Bio-Rad, USA) and let to dry. Then, the membrane was incubated with a chromogenic substrate for horseradish peroxidase (0.4 mg/mL^{-1} 3-aminoethyl-9-carbazole in 0.5 M acetate buffer with 0.1% H_2O_2, pH 5.5), after the adequate development the reaction was stopped by rinsing with water. After drying the membranes were scanned according to the protocol mentioned in Krizkova et al. [77], in which function optical density (OD) of Biolight software (Vilber-Lourmat, France) was used for the calculation of dot volumes by contour recognition.

2.4 DNA experiments

DNA (1 mg/mL) in TE buffer (10 mM Tris-Hcl, 1 mM EDTA, pH = 7.5) was incubated for 3 h in dark at 4°C or under UV irradiation with addition of 0.1% H_2O_2 in flow-box. DNA purity was estimated spectrophotometrically (absorbance ratio 280/260 and 260/230 nm) using the UV–VIS spectrophotometer Specord 210 (Analytik Jena, Germany) and electrophoretically (1% agarose in TBE buffer (0.1 M Tris, 0.09 M boric acid, and 0.001 M EDTA) at 100 V for 60 min (Biorad, USA). Then, the aliquots of irradiated and non-irradiated DNA were digested by nuclease from *Staphylococcus* ssp. (1 U per 0.02 mg of DNA with addition of 1.64 mM $CaCl_2$ for 5 h at 37°C). 8-OHdG concentration in the samples was determined by ELISA.

2.5 Robotic pipetting station

For automated samples handling prior to their electrochemical analysis, an automated pipetting station Ep-Motion 5075 (Eppendorf, Germany) with computer controlling was used. Positions C1 and C4 were thermostated (Epthermoadapter PCR96). The samples can be placed in position B3 Ep 0.5/1.5/2 mL adaptor. In B1 position, Module Reservoir for washing solutions and waste were placed. Tips were placed in positions A4 (ePtips 50), A3 (ePtips 300) and A2 (ePtips 1000). Transfer was ensured by a robotic arm with pipetting adaptors (TS50, TS300, TS1000 – numeric labelling refers to maximal pipetting volume in μL) and a gripper for platforms transport (TG-T). The program sequence was edited and the station was controlled in pEditor 4.0. For sample preparation, two platforms were used: Thermorack for 24 × 1.5–2 mL microtubes (Position C3), which was used for storage of working solutions, 96-well DPW plate with well volume of 1000 μL (Position C1), which was thermostated. After the immunoseparation and enzymatic reaction, the magnetic particles were forced using Promega magnetic pad (Promega, USA) (position B4) and the solutions were transferred to a new DPW plate, in which 1-naphthol determination was performed.

2.6 Flow injection analysis-amperometric detection

The instrument for flow injection analysis with amperometric detection (FIA-ED) based on HPLC platform consisted of solvent delivery pump operating in the range of 0.001–9.999 mL/min (Model 582 ESA, Chelmsford, MA, USA), a reaction coil (1 m) and an electrochemical detector was used. The electrochemical detector includes one low volume (5 μL) flow-through analytical cell (Model 5040, ESA), which consisted of GC working electrode, hydrogen–palladium electrode as the reference electrode and auxiliary electrode, and Coulochem III (ESA) as a control module. The sample (10 μL) was injected by autosampler (model 542, ESA) using a 6-way injection valve. The data obtained were processed by the Clarity software (Version 3.0.04.444, Data Apex, Czech Republic). The experiments were carried out at 20°C. A GCE was polished mechanically by 0.1 μm of alumina (ESA) and sonicated at room temperature for 5 min using a Sonorex Digital 10 P Sonicator (Bandelin, Berlin, Germany) at 40 W [78, 79].

2.7 Stopped flow injection analysis – linear sweep voltammetry

The instrument for stopped flow injection analysis with electrochemical detection (SFIA-ED) consisted of solvent delivery automated analytical syringe operating in the working volume range of 1–50 μL under variable speed from 1.66 to 50 μL/s (Model eVol, SGE Analytical Science, Australia), 3-way 2-position selector valve (made from 6-way valve) (Valco, Instruments, USA), and dosing capillary that is directly entering to the electrochemical flow cell (CH Instruments, USA). The electrochemical flow cell includes one low volume (1.5 μL) flow-through analytical cell (CH Instruments), which consisted of doubled GC working electrode, Ag/AgCl electrode as the reference electrode and output steel tubing as an auxiliary electrode. Electrochemical flow cell was connected to miniaturize-potentiostat 910 PSTAT mini (Metrohm, Switzerland) as a control module. The sample (10 μL) was injected by automated syringe (SGE Analytical Science, Australia) through flow cell in speed of 1.66 μL/s. The flow cell was cleaned by rinsing of 200 μL ethanol in water (75% *v*/*v*), then 200 μL of 100% methanol and stabilized by 200 μL of supporting electrolyte. Cleaning was applied after 50 measurements. The data obtained were processed by the PSTAT software 1.0 (Metrohm, Switzerland). The experiments were carried out at 20°C. Other experimental parameters were optimized; see in Section 3.

2.8 Real samples – cancer patients

Samples obtained from 14 patients were used in our experiments. Age of patients ranged from 48 to 78 years with an average of 62.7 years and median of 59 years. Histologically, all patients had acinar adenocarcinoma of varying degrees of differentiation. None of the patients had metastases in local lymph nodes or in distant lymph nodes, bones, or in another location. Bioptic and histological examinations and routine biochemical tests were performed at Department of Pathological Physiology, Faculty of Medicine, Masaryk University, Czech Republic. Urine of the patients was centrifuged at $4000 \times g$ for 10 min. The samples were stored in -20°C prior to analysis. Collecting of the samples was approved by Ethical commission of Faculty Hospital in Brno.

2.9 Descriptive statistics

Data were processed using MICROSOFT EXCEL® (USA) and STATISTICA.CZ Version 8.0 (Czech Republic). The results are expressed as mean $\pm$ SD unless noted otherwise. The detection limits (3 signal/noise, S/N) were calculated according to Long and Winefordner [80], whereas N was expressed as standard deviation of noise determined in the signal domain unless stated otherwise.

3 Results and discussion

The complexity of biological matrix for determination of 8-OHdG demands few-steps sample preparation prior to analysis as it has been shown [81–83]. Using paramagnetic beads for 8-OHdG immunoextraction and immunodetection reduces the samples processing and therefore minimizes the risk of artefacts. Primarily, we tested antibodies function by ELISA according to the previously published papers [84, 85]. Then, we verified determination of 8-OHdG in differently damaged DNA [83, 86]. After that basic verifications we were prepared to start with optimization of paramagnetic particle-based immunoseparation. The optimization was carried out using automated pipetting station, which was individually programmed for each specific testing sequence. Samples prepared were immediately analyzed by SFIA-ED system and data were statistically processed.

3.1 ELISA detection of 8-OHdG

In this study, a standard ELISA-based method for determination of 8-OHdG with possibility to apply this method on paramagnetic particles was tested (Fig. 1). Polyclonal goat anti-8-OHdG antibodies diluted 1:10000 in 0.05 M carbonate buffer (0.032 M Na_2CO_3 and 0.068 M $NaHCO_3$, pH 9.6) were adsorbed on a polystyrene 96-well microplate. BSA was used to block free surface of the wells. Further, the plate was washed, and then 8-OHdG was applied. After the washing, the plate was incubated with mouse anti-8-OHdG primary antibody and, after that, the plate was incubated with AP-conjugated rabbit anti-mouse IgG to visualize the interaction of 8-OHdG with the primary antibody (Fig. 1Ba). According to this scheme, various concentrations of 8-OHdG were tested (Fig. 1Bb). The measured signal enhanced with increasing concentration of target molecule linearly with $R^2 = 0.985$ in the interval from 12.5 to 400 ng/mL. To verify the applicability of the method, test the ability of the system to detect DNA oxidation was performed. UV-irradiated oxidized DNA was prepared. DNA (1 mg/mL) was oxidized with H_2O_2 and UV-irradiated (called ''oxidized'') for 3 h. Control DNA (called ''native'') was stored in dark at 4°C for the same time. Both DNA samples were measured spectrophotometrically and electrophoretically. Agarose gel electrophoresis confirmed DNA degradation in oxidized DNA (Fig. 1A). Spectrometric measurements revealed that 260/280 absorbance ratio was app. 1.75 for both DNA samples and 260/230 absorbance ratio was 1.65 for native DNA and 0.99 for oxidized DNA. The decrease in the signal can be associated with the oxidation lesions in DNA. ELISA was used to confirm this assumption by determination of 8-OHdG. Both DNA samples were measured in normal and then in digested state, which was carried out by nuclease from *Staphylococcus* ssp. The highest signal was determined in oxidized and digested DNA followed by native and digested DNA. Among non-digested samples, signal measured in non-digested and oxidized DNA sample was higher compared to non-digested and native one (Fig. 1Bc). The differences between native and oxidized DNA was higher in non-digested samples. After digestion with staphylococcal nuclease the difference between irradiated and non-irradiated DNA was app. 15% (Fig. 1Bc). This may be caused due to the cross-reactivity of antibodies with other nucleotides or further DNA oxidation during the enzymatic reaction. To estimate the cross-reactivity, 0, 4, 40 and 400 ng/mL of 8-OHdG was mixed with mixture of DNA nucleotides (1.41 μM adenine, thymine, cytosine and guanosine, i.e. equimolar to 400 ng/mL 8-OHdG). Determined 8-OHdG concentrations were 395.6 and 41.7 ng/mL. 8-OHdG content on the sample containing 4 ng/mL of the analyte was out of the linear range, but even for this concentration the signal intensity was app. 5% higher than the signal of nucleotides mixture (Fig. 1Bb). The obtained results indicate that the suggested system is capable to detect 8-OHdG both in DNA and in nucleotides mixture. To decrease the detection limit and reduce the analysis time, this system was adopted for automated 8-OHdG analysis using magnetizable microparticles and robotic pipetting station.

3.2 Basic experimental scheme

Magnetic particles and nanoparticles can be used for numerous applications including those important in clinical diagnostics as early detection of serious diseases through detection of disease markers [87, 88]. The main aim of this

study was to design an approach based on immunoseparation of 8-OHdG (Fig. 1Ca) as a compound of interest.

To automate ELISA-based immune separation and detection of 8-OHdG, paramagnetic particles with covalently bound protein G were used. Magnetic particles were modified with two concentrations of goat anti-8-OHdG diluted in PBS as 1:4000 and/or 1:8000 (1 h, 37°C). Then 8-OHdG in concentrations of 0 and 25 ng/mL was added (1 h, 37°C). After the incubation with 8-OHdG, the particles were incubated with mouse anti-8-OHdG antibody (30 min, 37°C) and, after the washing, rabbit anti-mouse secondary antibody conjugated with horseradish peroxidase was applied (30 min, 37°C) (Fig. 1Cb). For rapid testing of usability of this system on microparticles, dot blot with 8-OHdG standard using magnetic particles was carried out. The sample was pipetted onto a PVDF membrane (Biorad) and dried at room temperature. Then the membrane was incubated in a chromogenic substrate for HRP (3-amino-ethyl-9-carbazole). Colour changes are shown in Fig. 1Cc. Magnetic particles without 8-OHdG gave negligible colour, which is probably associated with non-specific interactions of secondary antibody with magnetic particles surface. Other experimental parameters will be published elsewhere.

3.3 Modification of paramagnetic particles with antibodies by microfluidic robotic station

Based on the above-mentioned results it can be concluded that paramagnetic-based immunoseparation can be used for determination of 8-OHdG. However, due to colour product detection, miniaturization without loss of sensitivity could be difficult. 1-Naphthol generated by alkaline phosphatase from 1-naphthylphosphate is beneficial for electrochemical detection in miniaturized systems [89, 90]. This molecule provides very good electrochemical response across of various electrochemical methods, which can be used for its determination [91]. Electrochemical detector with a GC working electrode provides potential in further miniaturization and robustness [92–95]. Due to this fact and based on the previously mentioned steps, the particles were modified according to the scheme shown in Fig. 2A in order to optimize the electrochemical detection of 1-naphthol. Robotic station allowing modification of the paramagnetic particles without human handling was used for all pipetting, separation and incubation steps. AP-conjugated rabbit anti-mouse IgG was coupled to paramagnetic particles modified with recombinant protein G. The enzyme cleaved phosphate from the 1-naphthylphosphate forming electroactive 1-naphthol (Fig. 2A), which was then offline detected by SFIA-ED (Fig. 2B).

3.4 Microfluidic system with electrochemical detection in connection with magnetic particles

Microfluidic system for fully automated electrochemical detection was suggested (SFIA-ED, Fig. 3). The system composed of programmed syringe pump, switching valve and a prototype of miniaturized micropotentiostat (Fig. 3D). Programmed syringe pump enables precise sample injections (units of μL with error lower than 5%). To prepare a fully automated system, switching valve enabling switching between the off waste and sample flow was placed into the system. Flow cell in volume of 500–1000 nL with electrochemical detector (working electrode: GCE, auxiliary electrode: platinum, referent electrode: Ag/AgCl 3 M KCl) was used for detection (Fig. 3B and C). Prototype of miniaturized micropotentiostat for electrochemical detection was used in the suggested SFIA system (Fig. 3D and E). The suggested microfluidic arrangement was verified in terms of its functionality, repeatability and robustness. During the detailed testing of the system by measuring 1-naphthol concentration under optimized conditions (Section 3.4), variations in the sample volumes not greater than the following ones were observed: 4.5% interday ($n = 50$) and intraday (in day intervals 1–4.7%, 2–4.9%, 4–5.1%, 6–5.7%, ($n = 10$)). The suggested solution meets the technical requirements needed for the analysis of environmental and clinical samples [96, 97].

3.5 Study of basic electrochemical behaviour of 1-naphthol by using SFIA-ED

Suggested microfluidic device was used to study the electrochemical behaviour of 1-naphthol. Supporting electrolyte for electrochemical detection of 1-naphthol was used based on the results published by Palecek et al. [91]. Primarily, we made basic comparison of our designed low pressure SFIA system working in reversed mode with high-pressure platform FIA coupled with electrochemical detector. We aimed our attention on the optimization of linear sweep voltammetric (LSV) method to obtain the best conditions for 1-naphthol detection. Cyclic voltammograms for both detection cells using a same potentiostat (PSTAT mini) and all conditions as mobile phase (carbonate buffer), sample concentration (1-naphthol, 10 μg/mL) and sample dose (10 μL) are shown in Fig. 4. Cyclic voltammograms at three different scan rates (5, 10 and 15 mV/s) using GCE (Fig. 4Aa) and ESA electrochemical cell (Fig. 4Ba) were measured. It clearly follows from the results obtained that GC electrode gave better developed signals of 1-naphthol at app. 370 mV compared with ESA and dependence of their heights on scan rate measure on this electrode was linear up to 20 mV/s with $R^2 = 0.98$ (Fig. 4Ab). Higher scan rates did not enhance the signal Dependence of 1-naphthol signal height on scan rate measured by using of ESA electrochemical cell was also linear $R^2 = 0.99$ (Fig. 4Bb). The signal shifted to more positive potentials with increasing potential for 30 mV per 5 mV/s of the scan rate (Fig. 4Bb).

The obtained parameters were used in the following experiments for optimization of SFIA-ED conditions. First, the sample injection was optimized (Fig. 5A). Tested

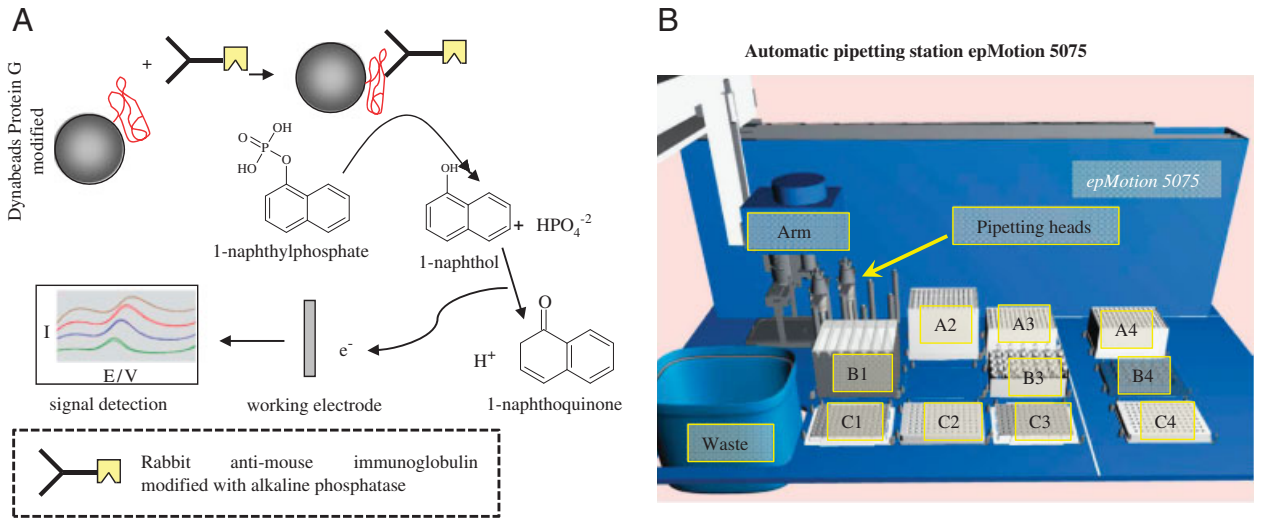

Figure 2. AP-conjugated rabbit anti-mouse IgG was coupled with protein G covalently immobilized to the surface of the magnetic particles. Alkaline phosphatase cleaves 1-naphthylphosphate forming 1-naphthol and hydrogenphosphate. 1-Naphthol was detected electrochemically (linear scan voltametry) (A). Scheme of automatic pipetting station epMotion 5075: A2, A3, A4 position on tips, B1 dispenser with washing solutions, and waste, B3 dispenser for antibodies and substrate, B4 magnetic stand, C1 thermostated position (4°C), C2 a C4 manipulation positions, C3 thermostated position (37°C) (B).

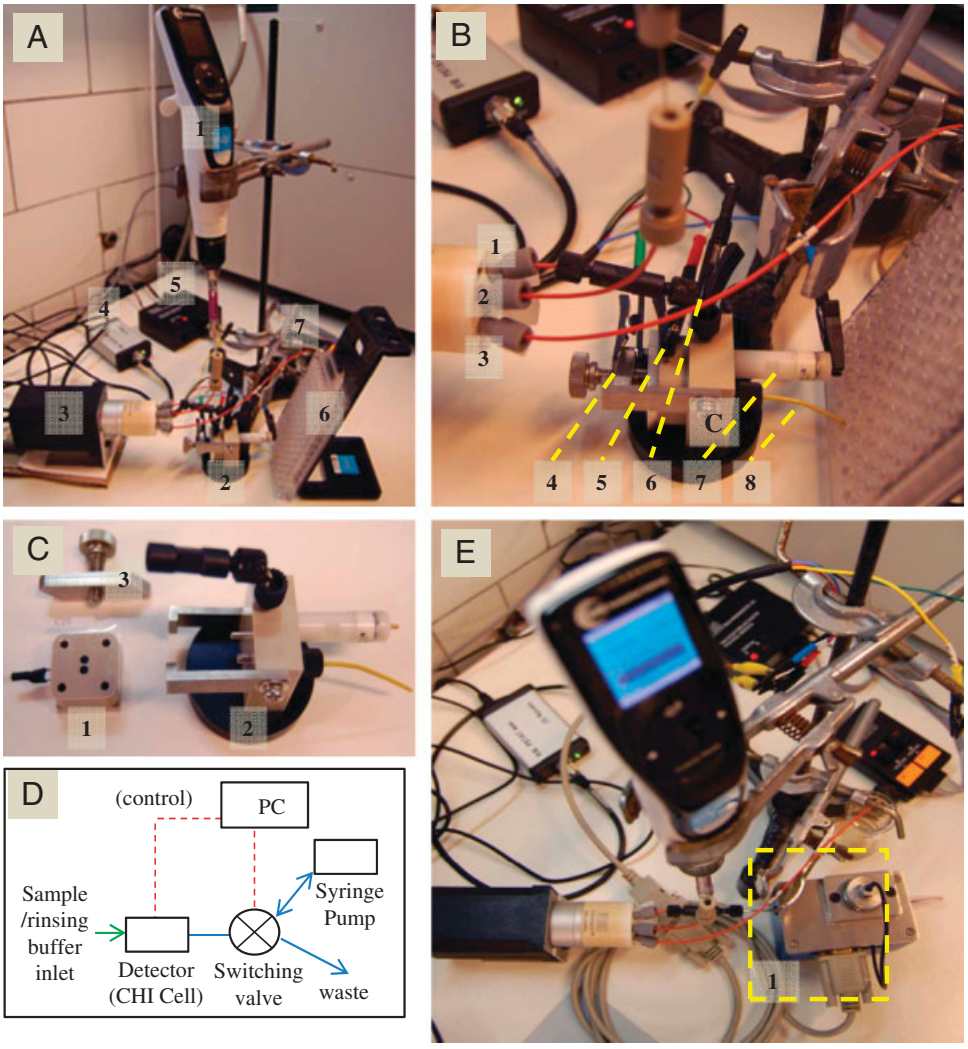

Figure 3. Photo of SFIA instrument (1-syringe pump, 2-flow cell, 3-switching valve, 4-potentiostat, 5-valve control, 6-microtiter plate, 7-waste (A). Photo of switching valve, flow cell and sample inlet in detail (1-flow cell port, 2-syringe port, 3-waste port, 4-ground, 5-working electrode, 6-auxiliary electrode, 7-referent electrode, 8-sample capillary) (B). Detail on flow cell (1-working electrode, 2-flow cell body, 3-working electrode fixture) (C). Scheme of SFIA instrument (D). SFIA instrument in connection with Analytical cell 5040 (E).

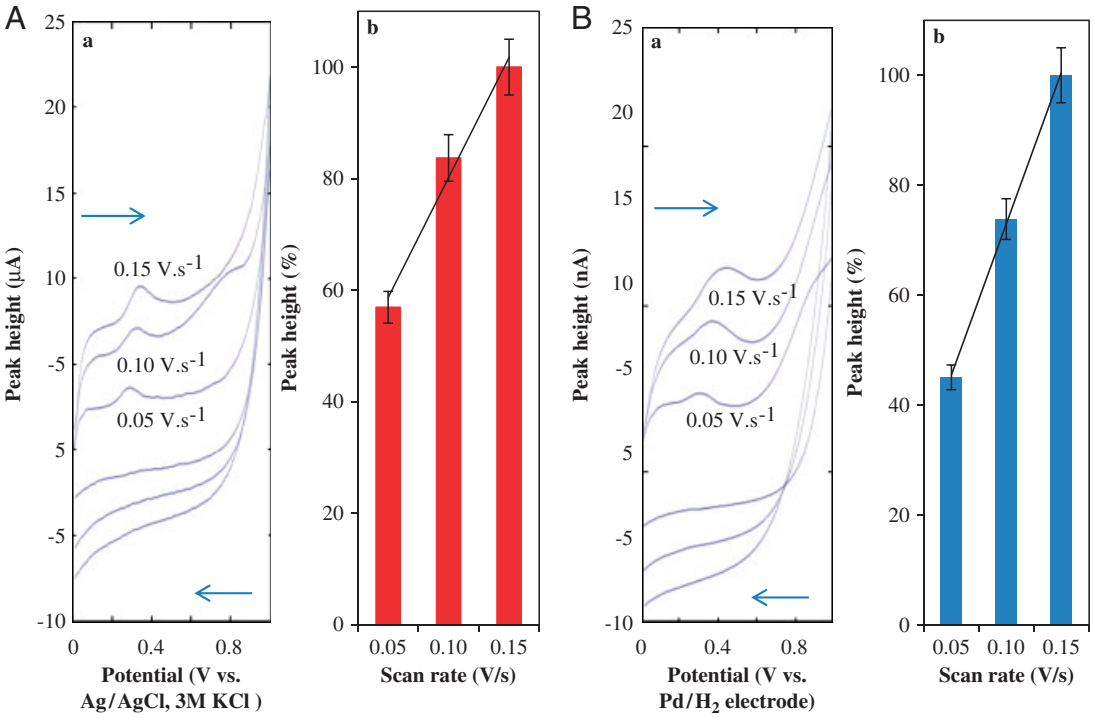

Figure 4. Cyclic voltammetry of 1-naphthol 100 pg/injection in carbonate buffer pH 9.6. Applied scan rate 50, 10, 15 and 20 mV/s. Electrochemical conditions: start of scan 0 V to vertex potential 1.0 V and end potential 0 V, potential step 5 mV. GC electrode cell with reference electrode Ag/AgCl 3MKCl (Aa). Dependence of 1-naphthol signal height on scan rate (Ab). Cyclic voltammetry of 1-naphthol 100 pg/injection in carbonate buffer pH 9.6. Applied scan rate 50, 10, 15 and 20 mV/s. Electrochemical conditions: start of scan 0 V to vertex potential 1.0 V and end potential 0 V, potential step 5 mV. GC electrode cell with reference electrode Ag/AgCl 3MKCl GC electrode cell 5040 with reference electrode PdH (Ba). Dependence of 1-naphthol signal height on scan rate (Bb).

interval of injection was from 2 to 16 μL. We found that application of more than 10 μL of a sample into the system did not cause any enhancement of the signal height (Fig. 5A). The maximal analysing sample volume (10 μL) was given by the total cell volume plus volume of dosing capillary and volume of output steel tube serving as referent electrode. Based on the experimental data obtained it clearly follows that volume of sample as 8 μL was sufficient for filling of the electrochemical cell. In the case that a sample is injected with buffer into the system, minimal sample volume of 5 μL is needed for repeatable measurements (relative standard deviation (RSD) 5.9%, $n = 10$). Under lower injecting volumes, RSD rapidly increased due to dilution of a sample by buffer (RSD 10.9%, $n = 10$). Moreover, we tested electrochemical cell 5040 with larger volume (5 μL) and active surface of GC into which 10 μL of various concentrations of 1-naphthol was dosed. The measured dependence was strictly linear as $y = 10.677x + 40.585$, $R^2 = 0.9954$ with detection limit of 360 fg of 1-naphthol per 5 μL injection (Fig. 5B). Based on these data, the optimization of previously used miniaturized cell followed. Working electrode condition was the other optimized parameter. Dependence of of 1-naphthol (100 pg/injection) signal on time of electrode conditioning is shown in Fig. 5C. It clearly follows from the results obtained that shorter electrode conditioning (within interval from 10 to 15 s) enhanced electrochemical signal of the target molecule. Moreover, potential of 1-naphthol signals shifted to more positive values with increasing time of electrode conditioning for 10 mV per 10 s of the conditioning (Fig. 5D). In addition, we tested number of repeated injections with purification of the electrode surface. It was found that we were able to carry out up to 4 repeated measurements of 1-naphthol with sufficient RSD as 8.8% ($n = 5$). Higher number of measurements without purification led to enhancement of the deviation up to 40%. The optimal chemical purification of GC electrode surface per four measurements was as follows: 20 μL 5% methanol, 10 μL 5% ethanol and 20 μL carbonate buffer. Under these conditions, 100 pg of 1-naphthol per injection was detected with good repeatability as RSD = 9.3%, $n = 10$. Further, the calibration dependence of 1-naphthol was measured (Fig. 5E). The shape of the response curve was exponential in tested concentration range from 0.2 to 200 pg of 1-naphthol per injection. For analytical purposes, we attempted to divide the concentration interval into two parts in order to utilize both of them. The lower one within the interval from 0.2 to 8 pg of 1-naphthol per injection is shown in inset in Fig. 5E. The calibration curve was strictly linear $y = 200.83x + 30.582$, $R^2 = 0.9904$; RSD = 9.3%, $n = 10$.

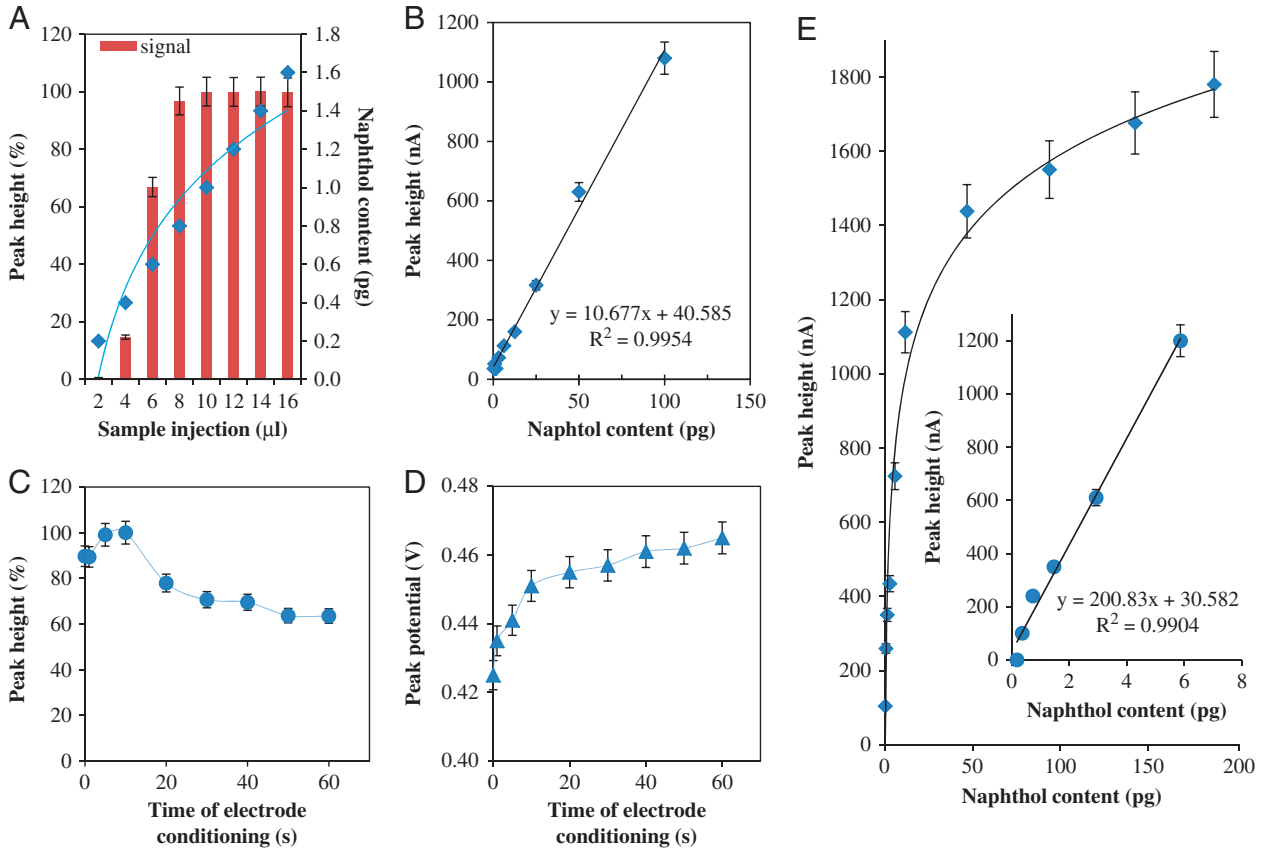

Figure 5. Change in the electrochemical response of 1-naphthol in dependence on sample injection (A). Dependence of the electrochemical response of 1-naphthol on its concentration, measured on GC electrode cell 5040 with reference electrode PdH (B). Change in the 1-naphthol peak height (C) and potential (D) with increasing time of electrode conditioning. Change of the signal height in dependence on 1-naphthol concentration (0–200 pg/injection), in inset 0–8 pg/injection on GC electrode cell with reference electrode Ag/AgCl 3MKCl, LSV parameters: start of scan −0.5 V end of scan 1.5 V, scan rate 0.15 V/s, conditioning time 10 s et −0.5 V. For other experimental conditions see Fig. 4.

Detection limit (3 S/N) was estimated as 100 fg of 1-naphthol per 5 µL injection.

3.6 Offline SFIA electrochemical detection of 1-naphthol obtained from paramagnetic particles modified with AP-conjugated rabbit anti-mouse IgG

Magnetic particles modified by AP-conjugated rabbit anti-mouse IgG prepared according to scheme shown in Fig. 2A produce 1-naphthol in the presence 1-naphthylphosphate as a substrate. The product of this enzyme reaction can be subsequently detected by above optimized SFIA-ED (Fig. 5). Robotic system fully ensured transfer and handling of all chemicals needed for immobilization of antibody, washing and substrate dosage. Program of robotic preparation of paramagnetic particles was as follows: (i) washing paramagnetic particles (10 µL of sample) in PBS buffer (pH 7), (ii) immobilization of antibody onto the surface of paramagnetic particles, (iii) five times repeated washing of non-specifically bound of antibodies onto the surface of paramagnetic particles, (iv) adding of 1-naphthylphosphate, incubation at different temperatures, (v) sampling of 1-naphthol without paramagnetic particles. In addition, conditions to obtain the highest yield of 1-naphthol and the fastest sample preparation were optimized. Dependence of 1-naphthol signal height on time of incubation of AP-conjugated rabbit anti-mouse IgG (RAM-AP) at 30°C is shown in Fig. 6A. The maximal yield of the enzyme reaction was obtained after 30 min long incubation even under non-optimized conditions. Further, we studied the influence of dilution of the antibody (1:500, 1:1000, 1:2000, 1:4000 and 1:8000 with PBS) used for immobilization on the surface of the particles, on 1-naphthol signal (Fig. 6B). It clearly follows from the results obtained that dilution of the antibody of 1:500 gave the highest signal of 1-naphthol.

The advantage of this dilution is probably the perfect surface coverage of magnetic particles and to prevent any further steric inhibition of enzyme reactions. In the case that the influence of different substrate concentrations (1-naphthylphosphate) on the 1-naphthol signal height was studied at 30 min long incubation of this substrate in the

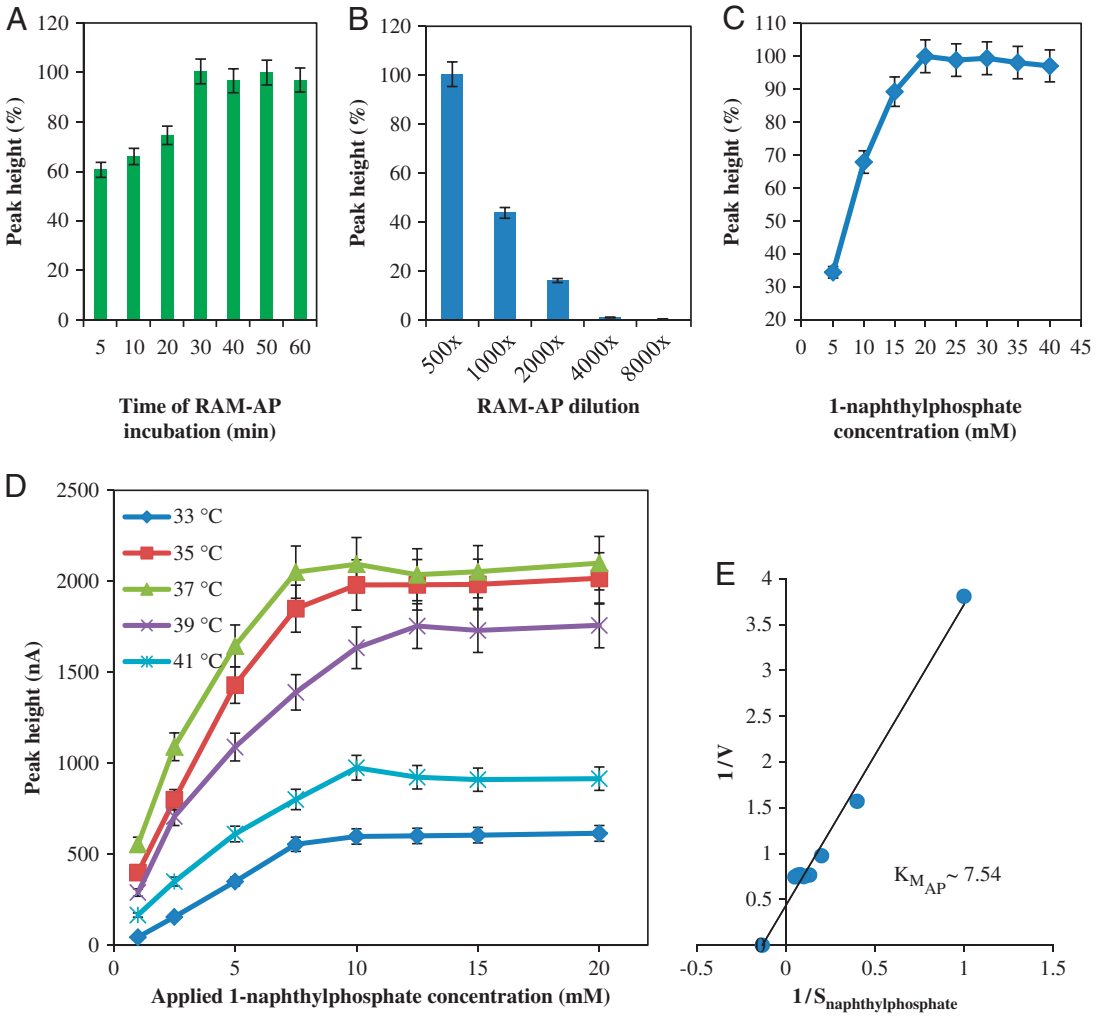

Figure 6. Change in the electrochemical response of 1-naphthol after incubation of 20 μL of microparticles modified with AP-conjugated rabbit anti-mouse immunoglobulins with 20 mM 1-naphthylphosphate for 5, 10, 20, 30, 40, 50 and 60 min, temperature 30°C, each measurement was repeated three times (A). Effect of dilution (1:500, 1:1000, 1:2000, 1:4000, 1:8000) of AP-conjugated rabbit anti-mouse antibody, time of incubation 30 min, other conditions see in part A (B). Dependence of 1-naphthol signal on concentration of 1-naphthylphosphate, other experimental details see in part A, B (C). Characteristic of enzymatic reaction catalysed by AP-conjugated rabbit anti-mouse IgG immobilized on magnetic particles. Condition of detection Michealis–Menten constant: substrate concentration 10 mM, time of incubation 30 min, dilution of antibody 1:500, temperature 37°C (D). Changes 1-naphthol signal at microparticles modified with AP-conjugated rabbit anti-mouse antibody in dependence on incubation temperature (33, 35, 37, 39 and 41°C), for other experimental details see part D (E).

presence of particle modified with RAM-AP (1:500 dilution with PBS), the highest signal was determined within concentration interval from 12 to 20 mM using microfluidic electrochemical instrument. Further, the effect of temperature of incubation of RAM-AP with various concentrations of the substrate on 1-naphthol signal height was investigated. The measured dependencies are shown in Fig. 6D. It can be concluded that the signal enhanced with the increasing incubation temperature up to 37°C. Under higher temperature, the signal decreased. Temperatures higher than 50°C stopped the reaction (not shown). Based on the results obtained, the enzyme kinetics of alkaline phosphatase coated on the surface of paramagnetic particles was estimated. The results are shown in Fig. 6E. Michaelis–Menten constant was found as $K_M = 7.54$ mM under the above optimized conditions, which shows on good affinity of enzyme to substrate.

3.7 Detection of 8-OHdG by using paramagnetic particles and SFIA-ED

Above-mentioned robotic programme was modified for immunodetection of 8-OHdG. (i) Magnetic particles (10 μL) were three times washed in PBS buffer (100 μL); (ii) goat immunoglobulin was bound on the surface of the particles modified with protein G for 60 min, dilution 1:500, at 37°C; (iii) washing step with PBS buffer (200 μL, five times

repeated); (iv) in order to prevent non-specific interaction, the free surface of the particles was blocked with 100 μg/mL of non-specific human immunoglobulin for 30 min at 37°C; (v) after washing step with PBS buffer (200 μL, five times repeated) various concentrations of 8-OHdG were incubated for 30 min at 37°C; (vi) after washing step with PBS buffer (200 μL, five times repeated) primary monoclonal mouse antibody anti-8-OHdG (dilution: 1:500) was incubated for 30 min at 37°C; (vii) after washing step with PBS buffer (200 μL, five times repeated) AP-conjugated rabbit anti-mouse IgG (dilution 1:500) was incubated for 30 min at 37°C; (viii) 1-naphthylphosphate (10 mM) was added and incubated

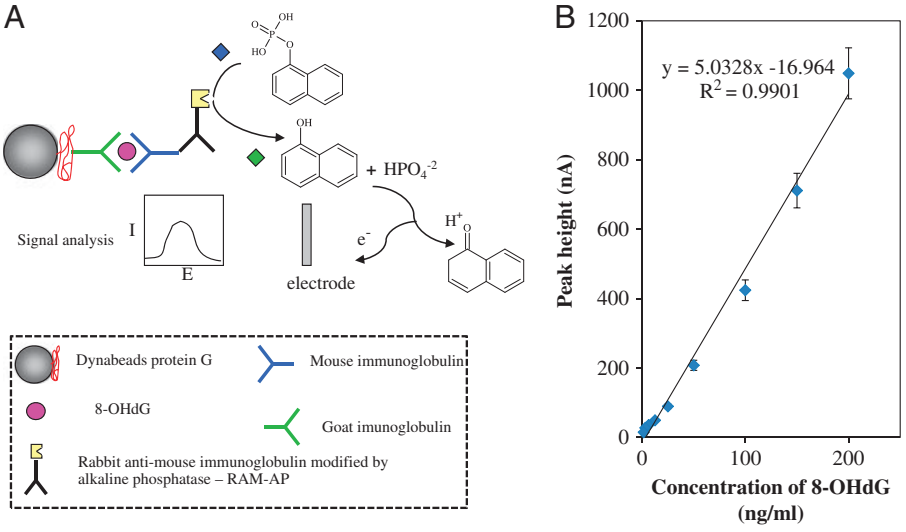

Figure 7. Simplified scheme of 8-OHdG detection. Polyclonal anti-8-OHdG goat immunoglobulins are coupled with protein G covalently attached to microparticles surface. After he blocking with non-specific immunoglobulins, the particles are incubated with a sample or 8-OHdG standard. Then a monoclonal mouse anti-8-OHdG antibody is bound to 8-OHdG. AP-conjugated rabbit anti-mouse antibody binds to the murine anti-8-OHdG antibody. Alkaline phosphatase cleaves 1-naphthylphosphate to 1-naphthol and hydrogenphosphate. 1-Naphthol is detected electrochemically (A). Typical dependence of 1-naphthol signal on 8-OHdG concentration (0–200 ng/mL).

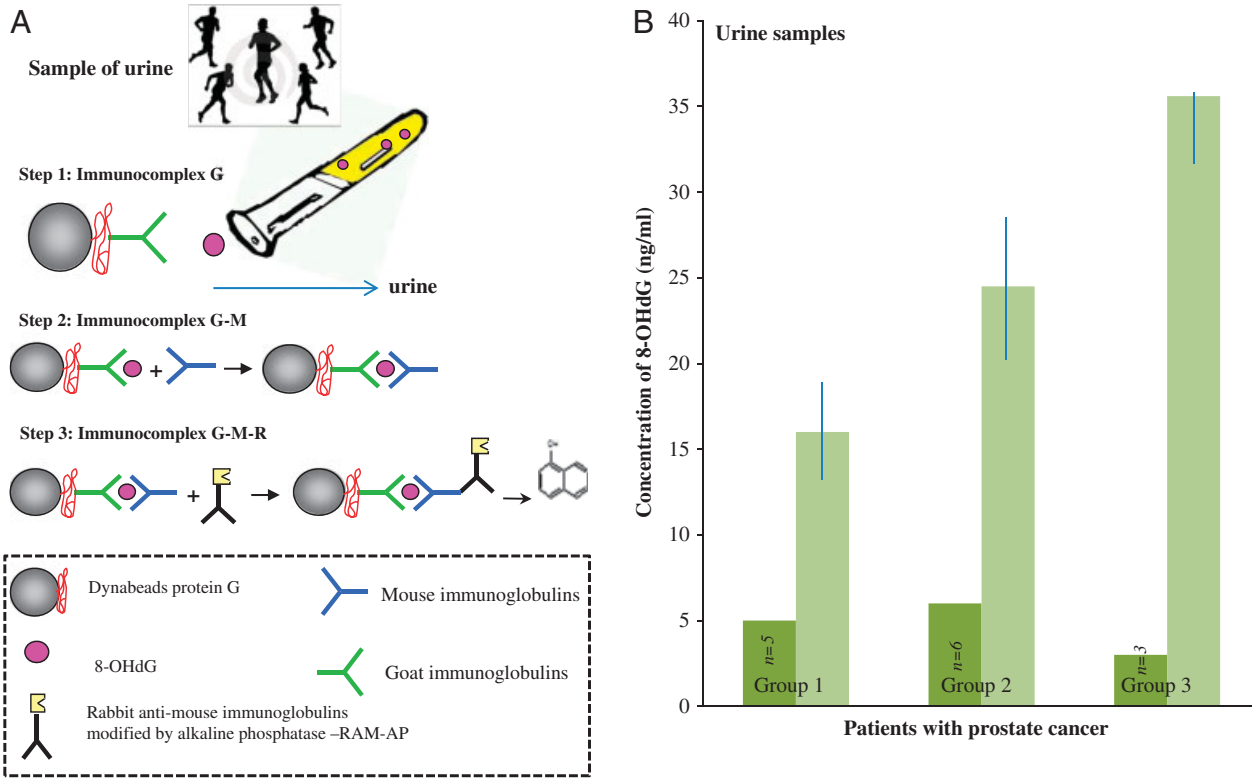

Figure 8. Simplified scheme of separation of 8-OHdG from urine samples. Step 1: Prepared immunocomplex G is incubated with the sample (urine) and the analyte is bound. Step 2: Formation of G-M immunocomplex. Step 3: Formation of G-M-R immunocomplex with consequent detection of 1-naphthol (A). Analysis of 8-OHdG concentration in urine samples of patients ($n = 14$) with prostate cancer. Dark column: number of samples, light column: average 8-OHdG concentration in group 1, 2 and 3. All experimental conditions are in Section 2.

for 20 min at 37°C; (ix) the sample for detection of 1-naphthol was obtained. The scheme of this procedure is shown in Fig. 7A. Total time of the preparation of solutions, modification of particles and detection of 1-naphthol did not exceed 6 h. Using the pre-coated and blocked particles reduce the time for analysis to 3 h. Taking account the possibility to prepare up to 96 samples and analyze them, the suggested approach markedly decrease time demands of the determination of 8-OHdG. Common ELISA methods are laborious and times for analysis vary from 3 to 16 h in dependence on experimental protocol. In addition, we were interested in the sensitivity of the method. Typical concentration-response curve measured within the interval from 0.25 to 200 ng/mL of 8-OHdG is shown in Fig. 7B. The dependence was linear in the tested concentration interval with the following equation $y = 5.03x - 16.96$, $R^2 = 0.9901$ (RSD = 8.9%, $n = 3$). Detection limit (3 S/N) was estimated as 5 pg/mL. The experiments verified that non-specific interactions with other immunoglobulins can be very effectively reduced by the addition of IgG as a blocking agent. In these experiments, negligible false positivity was observed in the sample without the presence of 8-OHdG. Moreover, detection of 8-OHdG in urine is influenced by interferences as uric acid and ascorbic acid, but the selective separation using antibodies eliminates the influence of these interferences substantially and in our experiment, we noticed no effect of these compounds on the signal of 8-OHdG.

3.8 Detection of 8-OHdG in patient with prostate cancer

Patients with cancer are exposed to considerable oxidative stress induced by both disease and the cancer treatment protocol [73, 74, 98–100]. Monitoring of the changes in levels of oxidative stress using easier and fully automated methodical approach could bring the immediate modification of treatment protocol to these patients (personalized medicine). The procedure of sample preparation is shown schematically in Fig. 8A. In the set of samples included in this study, three groups were recognized according to the concentration of urinary 8-OHdG. Group 1 with 8-OHdG concentration in the interval from 13 to 20 ng/mL) with average level as 16 ± 2 ng/mL; group 2 with 8-OHdG concentration in the interval from 21 to 30 ng/mL with average level as 25 ± 3 ng/mL and group 3 with 8-OHdG concentration higher than 31 ng/mL with average level as 36 ± 1 ng/mL were estimated (Fig. 8B). The highest frequency was observed in group 2 ($n = 6$). Detailed clinical study will be published elsewhere with regard to other clinical markers.

4 Concluding remarks

The presented results give a complex microfluidic approach for the detection of 8-OHdG based on highly selective monoclonal antibody capturing using modified paramagnetic particles. Analyte is electrochemically determined by the indirect detection of 1-naphthol using SFIA-ED. The whole process is designed as an offline system with minimizing human handling to reduce time of a sample analysis. It is expected that experimental design can be used for clinical application in the field personalized medicine.

Financial support from the grants CEITEC CZ.1.05/1.1.00/02.0068, NANOSEMED GA AV KAN20813081 and IGA MZ NS10200-3 is highly acknowledged.

The authors have declared no conflict of interest.

5 References

[1] Finkel, T., *Curr. Opin. Cell Biol.* 2003, *15*, 247–254.

[2] Finkel, T., Holbrook, N. J., *Nature* 2000, *408*, 239–247.

[3] Wu, L. L., Chiou, C.-C., Chang, P.-Y., Wu, J. T., *Clin. Chim. Acta* 2004, *339*, 1–9.

[4] Beckman, K. B., Ames, B. N., *J. Biol. Chem.* 1997, *272*, 19633–19636.

[5] Cooke, M. S., Evans, M. D., Dizdaroglu, M., Lunec, J., *Faseb J.* 2003, *17*, 1195–1214.

[6] Edge, R., Gaikwad, P., Navaratnam, S., Rao, B. S. M., Truscott, T. G., *Arch. Biochem. Biophys.* 2010, *504*, 100–103.

[7] Joergensen, A., Broedbaek, K., Weimann, A., Semba, R. D., Ferrucci, L., Joergensen, M. B., Poulsen, H. E., *PLoS One* 2011, *6*, e20795.

[8] Bahar, G., Feinmesser, R., Shpitzer, T., Popovtzer, A., Nagler, R. M., *Cancer* 2007, *109*, 54–59.

[9] Canakci, C. F., Canakci, V., Tatar, A., Eltas, A., Sezer, U., Cicek, Y., Oztas, S., *Arch. Immunol. Ther. Exp.* 2009, *57*, 205–211.

[10] Su, H. X., Baron, M., Benarroch, M., Velly, A. M., Gravel, S., Schipper, H. M., Gornitsky, M., *J. Rheumatol.* 2010, *37*, 1858–1863.

[11] Ni, Z. Y., Liu, Y. Q., Shen, H. M., Chia, S. E., Ong, C. N., *Mutat. Res.-Fundam. Mol. Mech. Mutagen* 1997, *381*, 77–82.

[12] Ishikawa, T., Fujioka, H., Ishimura, T., Takenaka, A., Fujisawa, M., *BJU Int.* 2007, *100*, 863–866.

[13] Nakamura, H., Kimura, T., Nakajima, A., Shimoya, K., Takemura, M., Hashimoto, K., Isaka, S., Azuma, J., Koyama, M., Murata, Y., *Eur. J. Obstet. Gynecol. Reprod. Biol.* 2002, *105*, 155–160.

[14] Chiou, C. C., Chang, P. Y., Chan, E. C., Wu, T. L., Tsao, K. C., Wu, J. T., *Clin. Chim. Acta* 2003, *334*, 87–94.

[15] Tokarz, A., Bobrowska, B., Kosk, M. G., *J. Food Lipids* 2008, *15*, 297–308.

[16] Yano, T., Shoji, F., Baba, H., Koga, T., Shiraishi, T., Orita, H., Kohno, H., *Lung Cancer* 2009, *63*, 111–114.

[17] Nagayoshi, Y., Kawano, H., Hokamaki, J., Uemura, T., Soejima, H., Kaikita, K., Sugiyama, S., Yamabe, H., Shioji, I., Sasaki, S., Kuroda, Y., Ogawa, H., *Free Radic. Res.* 2009, *43*, 1159–1166.

[18] Leinonen, J., Lehtimaki, T., Toyokuni, S., Okada, K., Tanaka, T., Hiai, H., Ochi, H., Laippala, P., Rantalaiho, V., Wirta, O., Pasternack, A., Alho, H., *FEBS Lett.* 1997, *417*, 150–152.

[19] Kikuchi, Y., Yasuhara, T., Agari, T., Kondo, A., Kuramoto, S., Kameda, M., Kadota, T., Baba, T., Tajiri, N., Wang, F. F., Tayra, J. T., Liang, H. B., Miyoshi, Y., Borlongan, C. V., Date, I., *J. Cell. Physiol.* 2011, *226*, 1390–1398.

[20] Nestorova, G., Zhang, C., Spaulding, J., Feng, J., *Free Radic. Biol. Med.* 2010, *49*, S79–S79.

[21] Wei, M., Wanibuchi, H., Morimura, K., Iwai, S., Yoshida, K., Endo, G., Nakae, D., Fukushima, S., *Carcinogenesis* 2002, *23*, 1387–1397.

[22] Valavanidis, A., Vlachogianni, T., Fiotakis, C., *J. Environ. Sci. Health Pt. C – Environ. Carcinog. Ecotoxicol. Rev.* 2009, *27*, 120–139.

[23] Yoshida, R., Ogawa, Y., Mori, I., Nakata, A., Wang, R. S., Ueno, S., Shioji, I., Hisanaga, N., *Mutagenesis* 2003, *18*, 533–537.

[24] Stiborova, M., Patocka, J., Frei, E., Schmeiser, H. H., *Chem. Listy* 2005, *99*, 782–788.

[25] Szymanska-Chabowska, A., Beck, A., Poreba, R., Andrzejak, R., Antonowicz-Juchniewicz, J., *Pol. J. Environ. Stud.* 2009, *18*, 1131–1139.

[26] Wang, H. M., Lv, S. H., Li, F. S., Liu, Q. A., Ke, S., *Sci. Total Environ.* 2010, *408*, 6092–6099.

[27] Valko, M., Morris, H., Cronin, M. T. D., *Curr. Med. Chem.* 2005, *12*, 1161–1208.

[28] Valko, M., Rhodes, C. J., Moncol, J., Izakovic, M., Mazur, M., *Chem. Biol. Interact.* 2006, *160*, 1–40.

[29] Yang, Y., Jin, X. M., Yan, C. H., Tian, Y., Tang, J. Y., Shen, X. M., *Toxicol. Ind. Health* 2008, *24*, 603–610.

[30] Colangelo, D., Mahboobi, H., Viarengo, A., Osella, D., *Biometals* 2004, *17*, 365–370.

[31] Chen, H. I., Liou, S. H., Ho, S. F., Wu, K. Y., Sun, C. W., Chen, M. F., Cheng, L. C., Shih, T. S., Loh, C. H., *J. Occup. Health* 2007, *49*, 389–398.

[32] Goyal, R. N., Oyama, M., Tyagi, A., *Anal. Chim. Acta* 2007, *581*, 32–36.

[33] Pilger, A., Rudiger, H. W., *Int. Arch. Occup. Environ. Health* 2006, *80*, 1–15.

[34] Koide, S., Kinoshita, Y., Ito, N., Kimura, J., Yokoyama, K., Karube, I., *J. Chromatogr. B* 2010, *878*, 2163–2167.

[35] Matsumoto, Y., Ogawa, Y., Yoshida, R., Shimamori, A., Kasai, H., Ohta, H., *J. Occup. Health* 2008, *50*, 366–372.

[36] Kasai, H., Svoboda, P., Yamasaki, S., Kawai, K., *Ind. Health* 2005, *43*, 333–336.

[37] Brett, A. M. O., Piedade, J. A. P., Serrano, S. H. P., *Electroanalysis* 2000, *12*, 969–973.

[38] Wan, C. D., Liu, T., Wei, S., Zhang, S. H., *Russ. J. Electrochem.* 2008, *44*, 327–331.

[39] Gutierrez, A., Gutierrez, S., Garcia, G., Galicia, L., Rivas, G. A., *Electroanalysis* 2011, *23*, 1221–1228.

[40] Langmaier, J., Samec, Z., Samcova, E., *Electroanalysis* 2003, *15*, 1555–1560.

[41] Prabhulkar, S., Li, C. Z., *Biosens. Bioelectron.* 2010, *26*, 1743–1749.

[42] Lin, C. C., Wang, J. H., Wu, H. W., Lee, G. B., *JALA* 2010, *15*, 253–274.

[43] Pumera, M., Merkoci, A., Alegret, S., *Trac – Trends Anal. Chem.* 2006, *25*, 219–235.

[44] Becker, C., Hodenius, M., Blendinger, G., Sechi, A., Hieronymus, T., Muller-Schulte, D., Schmitz-Rode, T., Zenke, M., *J. Magn. Magn. Mater.* 2007, *311*, 234–237.

[45] Cao, Z. J., Li, Z. X., Zhao, Y. J., Song, Y. M., Lu, J. Z., *Anal. Chim. Acta* 2006, *557*, 152–158.

[46] Chiou, C. H., Huang, Y. Y., Chiang, M. H., Lee, H. H., Lee, G. B., *Nanotechnology* 2006, *17*, 1217–1224.

[47] Jaffrezic-Renault, N., Martelet, C., Chevolot, Y., Cloarec, J. P., *Sensors* 2007, *7*, 589–614.

[48] Kim, D. K., Zhang, Y., Voit, W., Rao, K. V., Muhammed, M., *J. Magn. Magn. Mater.* 2001, *225*, 30–36.

[49] Kinoshita, T., Seino, S., Mizukoshi, Y., Nakagawa, T., Yamamoto, T. A., *J. Magn. Magn. Mater.* 2007, *311*, 255–258.

[50] Palecek, E., Fojta, M., *Talanta* 2007, *74*, 276–290.

[51] Yeung, S. W., Hsing, I. M., *Biosens. Bioelectron.* 2006, *21*, 989–997.

[52] Ngomsik, A. F., Bee, A., Draye, M., Cote, G., Cabuil, V., *C. R. Chim.* 2005, *8*, 963–970.

[53] Lund-Olesen, T., Dufva, M., Hansen, M. F., *J. Magn. Magn. Mater.* 2007, *311*, 396–400.

[54] Lunov, O., Bespalova, S., Zablotskii, V., *J. Magn. Magn. Mater.* 2007, *311*, 162–165.

[55] Hsing, I. M., Xu, Y., Zhao, W. T., *Electroanalysis* 2007, *19*, 755–768.

[56] Xu, C. J., Sun, S. H., *Polym. Int.* 2007, *56*, 821–826.

[57] Yu, C. H., Lo, C. C. H., Tam, K., Tsang, S. C., *J. Phys. Chem. C* 2007, *111*, 7879–7882.

[58] Huska, D., Adam, V., Trnkova, L., Kizek, R., *J. Magn. Magn. Mater.* 2009, *321*, 1474–1477.

[59] Huska, D., Hubalek, J., Adam, V., Vajtr, D., Horna, A., Trnkova, L., Havel, L., Kizek, R., *Talanta* 2009, *79*, 402–411.

[60] Musarrat, J., Wani, A. A., *Carcinogenesis* 1994, *15*, 2037–2043.

[61] Toyokuni, S., Tanaka, T., Hatton, Y., Nishiyama, Y., Yoshida, A., Uchida, K., Hiai, H., Ochi, H., Osawa, T., *Lab. Invest.* 1997, *76*, 365–374.

[62] Yin, B. Y., Whyatt, R. M., Perera, F. P., Randall, M. C., Cooper, T. B., Santella, R. M., *Free Radic. Biol. Med.* 1995, *18*, 1023–1032.

[63] Hamurcu, Z., Bayram, F., Kahriman, G., Donmez-Altuntas, H., Baskol, G., *Gynecol. Endocrinol.* 2011, *26*, 590–595.

[64] Patel, P. R., Bevan, R. J., Mistry, N., Lunec, J., *Free Radic. Biol. Med.* 2007, *42*, 552–558.

[65] Pan, H. Z., Chang, D., Feng, L. G., Xu, F. J., Kuang, H. Y., Lu, M. J., *Biomed. Environ. Sci.* 2007, *20*, 160–163.

[66] Huang, Y. J., Zhang, B. B., Ma, N., Murata, M., Tang, A. Z., Huang, G. W., *Med. Oncol.* 2010, *28*, 377–384.

[67] Jikimoto, T., Nishikubo, Y., Koshiba, M., Kanagawa, S., Morinobu, S., Morinobu, A., Saura, R., Mizuno, K.,

Kondo, S., Toyokuni, S., Nakamura, H., Yodoi, J., Kumagai, S., *Mol. Immunol.* 2002, *38*, 765–772.

[68] Thomson, C. A., Stendell-Hollis, N. R., Rock, C. L., Cussler, E. C., Flatt, S. W., Pierce, J. P., *Cancer Epidemiol. Biomarkers Prev.* 2007, *16*, 2008–2015.

[69] Breton, J., Sichel, F., Bianchini, F., Prevost, V., *Anal. Lett.* 2003, *36*, 123–134.

[70] Seki, S., Kitada, T., Yamada, T., Sakaguchi, H., Nakatani, K., Onoda, N., Satake, K., *Histopathology* 2002, *40*, 531–535.

[71] Kitada, T., Seki, S., Iwai, S., Yamada, T., Sakaguchi, H., Wakasa, K., *J. Hepatol.* 2001, *35*, 613–618.

[72] Won, M. H., Kang, T. C., Jeon, G. S., Lee, J. C., Kim, D. Y., Choi, E. M., Lee, K. H., Choi, C. D., Chung, M. H., Cho, S. S., *Brain Res.* 1999, *836*, 70–78.

[73] Karihtala, P., Kauppila, S., Puistola, U., Jukkola-Vuorinen, A., *Histopathology* 2011, *58*, 854–862.

[74] Pylvas, M., Puistola, U., Laatio, L., Kauppila, S., Karihtala, P., *Anticancer Res.* 2011, *31*, 1411–1415.

[75] Murtas, D., Piras, F., Minerba, L., Ugalde, J., Floris, C., Maxia, C., Demurtas, P., Perra, M. T., Sirigu, P., *Oncol. Rep.* 2010, *23*, 329–335.

[76] Labenski, M. T., Fisher, A. A., Tsaprailis, G., Monks, T., Lau, S. S., *Abstr. Pap. Am. Chem. Soc.* 2007, *234*, 1.

[77] Krizkova, S., Adam, V., Eckschlager, T., Kizek, R., *Electrophoresis* 2009, *30*, 3726–3735.

[78] Mikelova, R., Baloun, J., Petrlova, J., Adam, V., Havel, L., Petrek, J., Horna, A., Kizek, R., *Bioelectrochemistry* 2007, *70*, 508–518.

[79] Krizkova, S., Krystofova, O., Trnkova, L., Hubalek, J., Adam, V., Beklova, M., Horna, A., Havel, L., Kizek, R., *Sensors* 2009, *9*, 6934–6950.

[80] Long, G. L., Winefordner, J. D., *Anal. Chem.* 1983, *55*, A712–A724.

[81] Weiss, D. J., Lunte, C. E., *Electrophoresis* 2000, *21*, 2080–2085.

[82] Mei, S. R., Yao, C. H., Cai, L. S., Xing, J., Xu, G. W., Wu, C. Y., *Electrophoresis* 2003, *24*, 1411–1415.

[83] Wirtz, M., Schumann, C. A., Schellentrager, M., Gab, S., vom Brocke, J., Podeschwa, M. A. L., Altenbach, H. J., Oscier, D., Schmitz, O. J., *Electrophoresis* 2005, *26*, 2599–2607.

[84] Saito, S., Yamauchi, H., Hasui, Y., Kurashige, J., Ochi, H., Yoshida, K., *Res. Commun. Mol. Pat. Pharm.* 2000, *107*, 39–44.

[85] Shimoi, K., Kasai, H., Yokota, N., Toyokuni, S., Kinae, N., *Cancer Epidemiol. Biomarkers Prev.* 2002, *11*, 767–770.

[86] Dandona, P., Thusu, K., Cook, S., Snyder, B., Makowski, J., Armstrong, D., Nicotera, T., *Lancet* 1996, *347*, 444–445.

[87] Gupta, A. K., Naregalkar, R. R., Vaidya, V. D., Gupta, M., *Nanomedicine* 2007, *2*, 23–39.

[88] Chomoucka, J., Drbohlavova, J., Huska, D., Adam, V., Kizek, R., Hubalek, J., *Pharmacol. Res.* 2010, *62*, 144–149.

[89] Castanon-Fernandez, J., Fernandez-Abedul, M. T., Costa-Garcia, A., *Anal. Chim. Acta* 2000, *406*, 225–232.

[90] Moreno-Guzman, M., Gonzalez-Cortes, A., Yanez-Sedeno, P., Pingarron, J. M., *Anal. Chim. Acta* 2011, *692*, 125–130.

[91] Palecek, E., Kizek, R., Havran, L., Billova, S., Fojta, M., *Anal. Chim. Acta* 2002, *469*, 73–83.

[92] Huska, D., Hubalek, J., Adam, V., Kizek, R., *Electrophoresis* 2008, *29*, 4964–4971.

[93] Pumera, M., *Mater. Today* 2011, *14*, 308–315.

[94] Pumera, M., Escarpa, A., *Electrophoresis* 2011, *32*, 793–794.

[95] Scott, C. L., Pumera, M., *Electroanalysis* 2011, *23*, 858–861.

[96] Warsinke, A., Benkert, A., Scheller, F. W., *Fresenius J. Anal. Chem.* 2000, *366*, 622–634.

[97] Cerda, V., Estela, J. M., Forteza, R., Cladera, A., Becerra, E., Altimira, P., Sitjar, P., *Talanta* 1999, *50*, 695–705.

[98] Engstrom, K. S., Vahter, M., Johansson, G., Lindh, C. H., Teichert, F., Singh, R., Kippler, M., Nermell, B., Raqib, R., Stromberg, U., Broberg, K., *Free Radic. Biol. Med.* 2010, *48*, 1211–1217.

[99] Pylvas, M., Puistola, U., Kauppila, S., Soini, Y., Karihtala, P., *Eur. J. Cancer* 2010, *46*, 1661–1667.

[100] Whelan, K. F., Lu, J. P., Fridman, E., Wolf, A., Honig, A., Paulin, G., Klotz, L., Pinthus, J. H., *PloS One* 2010, *5*.

